Journal of Intelligent & Robotic Systems (2024) 110:32
https://doi.org/10.1007/s10846-024-02065-8

REGULAR PAPER

# Diving into Clarity: Restoring Underwater Images using Deep Learning

Laura A. Martinho[1] · João M. B. Calvalcanti[1] · José L. S. Pio[1] · Felipe G. Oliveira[1,2]

Received: 26 June 2023 / Accepted: 18 January 2024


## Abstract

In this paper we propose a learning-based restoration approach to learn the optimal parameters for enhancing the quality of different types of underwater images and apply a set of intensity transformation techniques to process raw underwater images. The methodology comprises two steps. Firstly, a Convolutional Neural Network (CNN) Regression model is employed to learn enhancing parameters for each underwater image type. Trained on a diverse dataset, the CNN captures complex relationships, enabling generalization to various underwater conditions. Secondly, we apply intensity transformation techniques to raw underwater images. These transformations collectively compensate for visual information loss due to underwater degradation, enhancing overall image quality. In order to evaluate the performance of our proposed approach, we conducted qualitative and quantitative experiments using well-known underwater image datasets (U45 and UIEB), and using the proposed challenging dataset composed by 276 underwater images from the Amazon region (AUID). The results demonstrate that our approach achieves an impressive accuracy rate in different underwater image datasets. For U45 and UIEB datasets, regarding PSNR and SSIM quality metrics, we achieved 26.967, 0.847, 27.299 and 0.793, respectively. Meanwhile, the best comparison techniques achieved 26.879, 0.831, 27.157 and 0.788, respectively.

**Keywords** Underwater image restoration · Deep learning · Learning-based image enhancement · Intensity transformation techniques

## 1 Introduction

Research work on underwater image restoration has been increasing in recent years and are extremely important for several applications in subaquatic robotics and scenarios. The acquisition process of good quality subaquatic images is a complex operation, representing a significant challenge for visual data capture and analysis, especially, due to the different underwater environments such as oceans, rivers and lakes [1–3]. Distinct aspects contribute to the mentioned challenging acquisition, including $i$) water turbidity, caused by suspended particles; $ii$) presence of marine organisms, that contribute to the degradation of image quality and water scattering; and $iii$) uneven lighting and optical distortion, resulting in reduced visibility and loss of details [4].

A wide range of applications demand the understanding and processing of underwater images, especially using subaquatic robots. In an industrial context, different uses can be found in underwater robotics, offshore engineering and underwater exploration, which require restored images for object detection and identification, navigation and situational awareness [5]. In a surveillance and monitoring context, the enhancement of underwater images, captured by subaquatic cameras and other sensors, enables the use of Remotely Operated Vehicle (ROV), assisting in wreck detection, threats and unauthorized objects and activities [6]. Finally, in a marine ecology and biology context, it is paramount to comprehend and monitor underwater ecosystems, allowing the identification of species and their behavior [7].

✉ Felipe G. Oliveira
felipeoliveira@ufam.edu.br

Laura A. Martinho
lam2@icomp.ufam.edu.br

João M. B. Calvalcanti
john@icomp.ufam.edu.br

José L. S. Pio
josepio@icomp.ufam.edu.br

[1] Contributing authors. Institute of Computing (ICOMP), Universidade Federal do Amazonas (UFAM), Manaus 69067-005, Brazil

[2] Institute of Exact Sciences and Technology (ICET), Universidade Federal do Amazonas (UFAM), Itacoatiara 69103-128, Brazil

Published online: 14 February 2024

Considering the underwater image acquisition complexity as mentioned earlier, the underwater image quality enhancement is a challenging problem, since there are many aspects affecting the subaquatic image quality. Additionally, the aforementioned real-world applications demonstrate the relevance of the addressed problem.

In order to tackle this problem, advanced algorithms and techniques have been proposed to compensate the adverse effects of light scattering and absorption. By employing such techniques, underwater images can be transformed to reveal fine details, high contrast and precise color representation. Several methods transforming the image intensities can be employed such as color and gamma correction, histogram and contrast adjustment and unsharp enhancement [4]. Figure 1 shows examples of raw underwater images, which were acquired in the ocean and in a river and their respective restored images.

In a previous work [8] we have proposed an approach to underwater image quality enhancement, applying a fusion of color adjustment and compensation techniques, reaching a reasonable performance in terms of visibility quality and image quality metrics scores. However, in that work, we have used a simple strategy where the parameters were manually adjusted.

In this paper we propose a Deep Learning-based approach for underwater image restoration, enhancing the quality and clarity of subaquatic images, improving the navigation capability of subaquatic robots. We use a Convolutional Neural Network (CNN) regression model to estimate the best parameters to reduce the image degradation. Next a sequence of intensity transformation techniques are applied using the parameters found by the CNN, in order to improve the subaquatic images quality. Experiments were carried out using two well-known underwater image datasets. We have also carried out a comparison of our results with other relevant state-of-the-art algorithms, such as VRE [9], UDCP [10], IBLA [11], CBF [12], GDCP [13], UWCNN (UCNN) [14], WaterNet (WN) [15] and LI [16]. The obtained results through qualitative and quantitative assessment metrics provide evidence supporting the effectiveness of the proposed approach for underwater image restoration, showcasing improved accuracy and significantly clearer underwater images. In the experiments, regarding the U45 and the UIEB datasets, seven state-of-the-art techniques were compared with our approach. For PSNR and SSIM quality metrics, in U45 dataset, the best results from comparison methods were 26.879 and 0.831, respectively. Meanwhile, our results were 26.967 and 0.847, respectively. For PSNR and SSIM quality metrics, in UIEB dataset, the best results from comparison methods were 27.157 and 0.788, respectively. Meanwhile, our results were 27.299 and 0.793, respectively. It is important to highlight that for PSNR and SSIM, the higher the value, the higher the restoration quality of underwater images.

Our work offers two main contributions, which can be summarized as follows:

- We propose a Deep Learning-based approach to learn the best parameters in the process of restoring the quality of underwater images. The proposed regression process acquires knowledge from different water conditions (like turbidity, low lighting, scattering and distortion in water), enabling the estimation of the better parameters for different underwater images. The proposed restoration approach presents high accuracy even regarding different water conditions. Thereby, our approach can improve the navigation capability of subaquatic robots in different underwater environments;
- We propose a challenging dataset composed by 276 underwater images, acquired in the Urubu river, a blackwater tributary of the Amazon river. The proposed dataset comprises subaquatic images with intense turbidity and low lighting and scattering in the water. To the best of our knowledge this is the first dataset of underwater images from the Amazon region.

The remainder of this paper is structured as follows. In Section II, we present a discussion about the most related works regarding underwater image processing and analysis. An overview of the proposed approach is presented in Section III, describing the main steps for the learning-based underwater image restoration technique. Real experiments

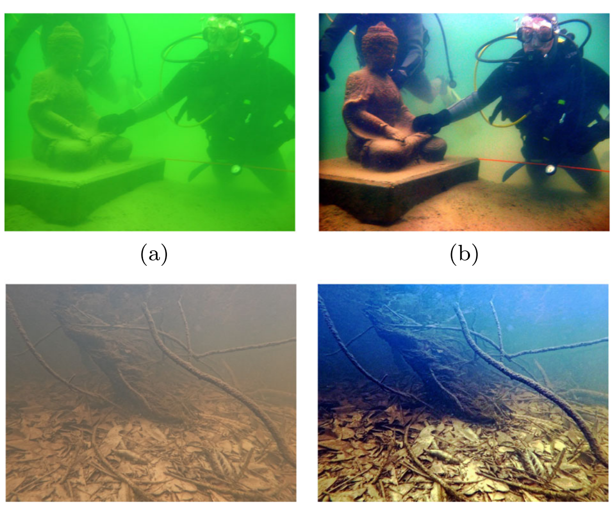

(a) (b) (c) (d)

**Fig. 1** Examples of raw and restored underwater images by our method. Figure 1a and b correspond to the raw and processed underwater images, respectively, in an ocean environment. Figures 1c and d correspond to the raw and processed underwater images, respectively, in a river environment are discussed in Section IV. Finally, in Section V we draw the conclusions and discuss paths for future investigation.

## 2 Related Work

Underwater image restoration has been the subject of intense research in the scope of subaquatic robotics and computer vision. This type of approach consists of enhancing the quality of subaquatic images to support real-world applications in different scenarios [17–19].

Several proposed state-of-the-art methods were designed to restore resolution of images to enhance visual perception by learning strategy. Zhangkai and Peng et al. [20] proposed a wavelet-based dual-stream network to solve color cast and blurry details in underwater images, using discrete wavelet transform added to frequency bands and two sub-networks: color and detail enhancement trying to reach a model that can effectively remove the color cast and improve the blurry details. In the same line of work, a high-performance underwater image enhancement model is proposed by Nianzu and Dong et al [21]. This approach is based on a deep learning network with multi-Scale and multi-dimensional feature to turbidity, light absorption, and scattering problem by a convolutional and pooling structure.

Many researches employ wavelet based strategies, including a two-step strategy based on color restoration and image fusion with deep learning and conventional image enhancement techniques [22]. This work uses an adaptive color compensation method and color restoration. A multi-stage deep Convolutional Neural Networks (CNN) framework with feature reconstruction loss and mean Squared Error is proposed by Sharma et al. [23], optimizing it using the traditional pixel-wise and feature-based cost functions. Liu et al. [24] proposed adaptive-learning techniques to remove color casts and low illumination and restore information, which proposed an adaptive learning attention network based on supervised learning named LaNet and Wang et al. [25] presented a reinforcement learning method with adaptive underwater presentation characteristics to improve image details.

The Retinex method is a technique widely used in the underwater field to improve color balance and lighting of images, increasing their visual quality. Zhenqi et al. [26] used rank learning and multi-scale dense Generative Adversarial Network (GAN) that leaded to a Retinex theory-based method to try boosting accuracy and robustness. Zhuang et al. [27] merged hyper-laplacian reflectance priors and retinex variational model to image enhancing.

Convolutional neural networks are used to enhance underwater images by removing fog and restoring color. Using an end-to-end defogging module and a brightness equalization module, Zheng et al. [28] proposes a CNN and an encoder-decoder backbone to color restoration. Liu et al. [29] work was also based on model image simulation, learning-based image enhancement with CNN and encoder-decoder backbone. However, some CNN approaches do not require encoders to color, contrast or dehaze underwater images, accomplishing improvement through multiscale densely connected deep CNN-based model, underwater optical imaging formulation and data-driven deep learning, as in Jiang et al. [30] method, or methods that uses medium transmission maps to restore real-world underwater images involving training a CNN using a GAN framework with dilated residual blocks (DRBs) [31].

Computer vision image fusion techniques can be applied in the underwater environment to combine and integrate different image sources. Zhao et al. [32] combined adaptive color compensation, improved Laplacian sharpening method, gamma correction, latent low-rank representation to dual-image weighted fusion. For detail preservation, Dhandapani et al. [33] worked on frequency domain model-free method, homomorphic filtering, discrete wavelet transform and fusion-based enhancement. MLLE (Minimal Color Loss and Locally Adaptive Contrast Enhancement) [34] can be performed in order to solve color correction, contrast enhancement with color transfer image generation based on minimum information loss principle and maximum attenuation map-guided fusion strategy for detail enhancement.

In the underwater context, super-resolution (SR) can help improve the visibility and clarity of the captured images. Improving image resolution, SR techniques [35] are based on deep learning models, CNN and multi-contextual formula, while Bapu et al. [36] proposed a method called Underwater Image Processing Scheme (UIPS), which utilizes Gradient Profile logic and image super-resolution norms to enhance the resolution and clarity of underwater images. FloodNet [37] achieved global feature fusion by low-level feature extraction and residual dense blocks, just as Li Wang et al. [38] providing image super-resolution and enhancement via progressive frequency-interleaved network, and U-Net [39] for simultaneous enhancement and super-resolution.

Image restoration through fusion of different techniques is a great way to achieve quality and detail gain in images, each technique providing its own quantitative parameter to process the capture. Wang et al. [40] joined parameter estimation by a three-channel cascade convolutional neural network (UTC-Net), while Shihao et al. [41] based research on deep learning to establish a neural network using dilated convolution and parameter correction. Turbid underwater image enhancement trough parameter-tuned stochastic resonance (PSR) can be good on effectively enhancing turbid underwater images without requiring prior assumptions or a large amount of data to be driven.

Our work proposes a new approach for the enhancement of underwater images, using a combination of processing

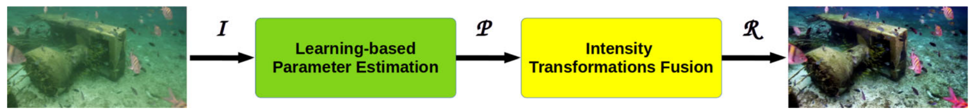


**Fig. 2** Overview of the proposed sequence of steps for underwater image restoration

techniques and convolutional neural networks (CNNs). This technique can be used in robotics vision applications such as search and rescue, surveillance and monitoring, and marine ecology and biology, improving the navigation in different scenarios such as oceans, rivers and lakes. This strategy aims to overcome the challenges when dealing with the limitations and distortions present in images captured in underwater environments. It is possible to identify several approaches that address the problem in a similar way to ours, including fusion processing techniques [32, 33], widely used to improve the quality and detail of images. It involves combining multiple images of the same scene, processed by different techniques, to produce a single high-quality image. As well as techniques using CNNs, neural networks specialized in image processing [23], capable of learning and extracting relevant features automatically [24]. Widely used in various computer vision tasks in the context of underwater image enhancement, CNNs can be trained to learn specific patterns of distortions and noise present in these images, with the goal of restoring the original quality.

## 3 Methodology

The proposed methodology is composed by two main steps: $i$) Learning-based Parameters Estimation; and $ii$) Intensity Transformation Fusion, as can be seen in Fig. 2, while further details will be presented in the next subsections. The first step consists of training a regression convolutional neural network, using a collection of raw underwater ($I$), to figure out the best parameters ($P$) for enhancing the quality of subaquatic images, regarding several scenarios and water conditions. The network analyzes the training image dataset and estimates the most efficient parameters for enhancing underwater images. Secondly, based on the identified optimal parameters, obtained from the learning process, intensity transformation functions are applied to restore the subaquatic images, resulting in enhanced underwater images ($R$).

### 3.1 Learning-based Parameters Estimation

For the Learning-based Parameters Estimation, first it was needed to correlate the underwater images with the best parameters for the intensity transformation functions. For this, an empirical process was performed in order to find out the best parameters to each raw underwater image. Finally, the pairs, comprising training raw subaquatic images and the best parameters found, are passed by the CNN regression training process.

Convolutional neural networks are a class of deep neural networks specially designed for processing structured data, such as images, performing a great role in image processing due to their ability to extract and automatically learn relevant features directly from data.

In our proposed method, the network is designed to estimate parameters of image processing techniques. This process consists of applying a CNN to estimate intensity variables resulting from a two-layer based enhancement method previously worked out [8]. Each proposed image processing step generates a numerical value for: color correction intensity ($cci$), gamma correction ($\gamma$), contrast intensity ($\beta$) and brightness intensity ($\alpha$).

The network generalizes the relationship between image features and parameters to obtain accurate estimates by being trained to learn complex patterns and relationships between input data and desired parameters. It learns to map image pixels to the optimal values of each parameter, enabling accurate estimation.

The proposed CNN model is composed by 3 convolutional layers, as shown in Fig. 3. The first layer is defined with 64 filters, the second and third layers are defined with 128 fil-

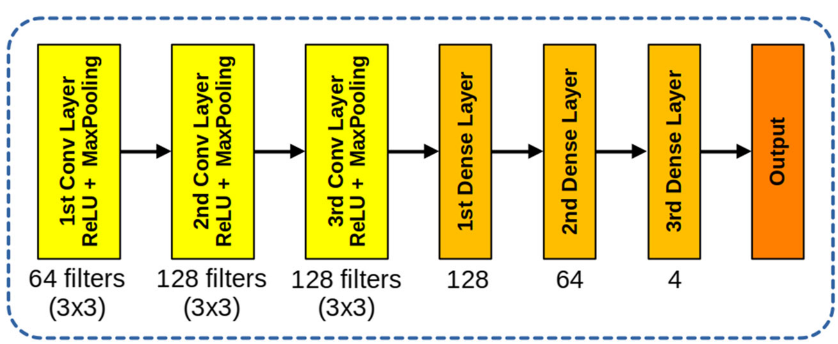


**Fig. 3** Proposed CNN architecture for underwater parameters estimation

ters. The filters size of all convolutional layers are (3x3). The ReLu activation function is used in all convolutional layers, altogether the Max Pooling function, regarding a window size of (2x2). After each convolution layer and after each Max Poling funcion a batch normalization is applied. After the convolutional layers, 2 fully-connected layers are proposed. The sizes of the fully-connected layers are 128 and 64, respectively for each flatten layer. Between each fully-connected layer are used Dropout layers with rate value of 0.5. The output dense layer of the model has 4 neurons corresponding to the 4 labels $(cci, \gamma, \alpha, \beta)$.

The goal is to adjust the weights of the neural network so as to minimize the loss function (mse) between the model predictions and the actual labels. In the training stage, the Adam optimization algorithm is used, with learning rate equal to 0.001. The training procedure was performed for 50 epochs and using a batch size of 128. The CNN regression model is used for underwater parameters estimation due to good results achieved in similar scenarios [14, 28, 35]. The proposed CNN model is also used due to good feature representation learning, depicting distinct and complementary features for modeling different underwater environments and water conditions.

In feature extraction, the proposed model figure out relevant features from the input images. This stage is performed by a series of convolutional layers, batch normalization and max-pooling layers. Mathematically, the feature extraction stage can be described as follows:

#### 3.1.1 Convolutional Layer

The input images are loaded and their labels are extracted from their filename. This layer is responsible for predicting the parameters, learning and identifying relevant visual patterns in the data, related to the predicted attributes.

$$Y = f(W * I + b) \tag{1}$$

Equation 1 shows the convolutional operation, where $I$ is defined as an input $64x64x3$ image, where $Y$ corresponds to the output feature map, $W$ the convolutional weights, $b$ the bias term and $f()$ corresponds to the activation function ReLU, represented as $f(x)$:

$$f(x) = \begin{cases} x, & \text{if} x > 0 \\ 0, & \text{otherwise.} \end{cases} \tag{2}$$

Through the convolutional layers, a hierarchy of feature detection occurs. Initial layers capture simple features such as lines and edges, deeper layers learn to combine these features into more complex textures and objects representations.

#### 3.1.2 Batch Normalization

Regarding the prediction of our parameters, Batch Normalization assists stabilizing the model training, allowing subsequent layers to benefit from normalized and more standardized inputs, resulting in more efficient and stable learning of relevant features in the underwater images, contributing to improved parameter predictions.

Let $Y_{normalized}$ be the normalized output, $m$ the input mean, $var$ its variance, $\epsilon$ a small number to avoid division by zero, $\beta$ and $\gamma$ the scaling and shifting parameters, respectively. The composing normalization operation was configured as below:

$$Y_{\text{normalized}} = \frac{Y - m}{\sqrt{var + \epsilon}} * \gamma + \beta. \tag{3}$$

#### 3.1.3 Max Pooling

The Max Pooling layer captures scale and location invariant features in the underwater images. It makes the model more robust to small variations in position and size of the features present in the images. This layer contributes to better parameter prediction, allowing the model to focus on the relevant information and generalize better to different underwater conditions.

$$Y_{pooled} = MaxPooling(Y_{normalized}), \tag{4}$$

where $Y_{normalized}$ is the output from batch normalization and $Y_pooled$ is the output feature map after pooling, both compose the max pooling operation.

The mentioned operations are repeated for multiple convolutional layers, with each layer extracting different features from the input image. The use of activation functions helps to introduce non-linearity and capture complex patterns in the data.

The goal of the feature learning stage is to further process the extracted features and learn higher-level representations that are relevant for the given task. In our method, this stage is performed by adding fully connected (dense) layers with dropout regularization.

#### 3.1.4 Flattening

Flatten layer provides a linear representation of the features extracted from the underwater images. This linear representation is then fed into the dense layers, which are responsible for learning the relationship between these features and making the final predictions.

The flattening operation, as shown in Eq. 5, where the output from the last max-pooling layer $(Y_{pooled})$ and the flattened vector representation of the features $(Y_{flattened})$ reshape a multidimensional input tensor into a one-dimensional vector.

$$Y_{flattened} = Flatten(Y_{pooled}) \tag{5}$$

#### 3.1.5 Fully Conected Layers

The Fully Connected layer performs linear and non linear transformations on the features extracted from the previous layers. It learns the relationship between these features and the parameters of interest, combining them in order to make accurate predictions. This layer plays a key role in the model's ability to learn complex, nonlinear patterns in the underwater images, contributing to the prediction of their parameters.

$$Y_{dense} = f(W * Y_{flattened} + b), \tag{6}$$

where $Y_{dense}$ is the output of the dense layer, $W$ the dense layer weights, $b$ the bias term and $f()$ corresponds to the activation function.

#### 3.1.6 Dropout Regularization

The dropout operation is composed by the output from the dense layer ($Y_{dense}$), output after dropout ($Y_{dropout}$) and the rate at which the neurons are randomly set to 0 during training (dropout_rate). This layer randomly disables a percentage of units during training, helping to avoid over fitting and co adaptation. It promotes the learning of more robust and independent features, improving the generalization of the model and contributing to the prediction of its desired parameters.

$$Y_{\text{dropout}} = \text{Dropout}(Y_{\text{dense}}, \text{dropout\_rate}), \tag{7}$$

where $Y_{dense}$ is the output of the dense layer, $W$ the dense layer weights, $b$ the bias term and $f()$ corresponds to the activation function.

#### 3.1.7 Final Output

Here, $Output$ represents the final output of the model, a Dense layer with 4 neurons to predict the desired parameters. It performs a linear transformation of the input data, adjusting the weights and biases to learn the relationship between the extracted features and the correct parameter values. This layer is important to predict the parameters by combining the previously extracted features and apply an appropriate activation function to map the final results to the desired parameter values.

Letting $W$ be the output layer weights, $Y_{dropout}$ represent the output after applying dropout, and $b$ represent the bias term, it is possible to finally show the final output of the model as:

$$\text{Output} = W \cdot Y_{\text{dropout}} + b. \tag{8}$$

The above operations are repeated for the specified number of epochs during training, optimized by the Grid Search, technique that allows you to find the best hyperparameters for a machine learning model by systematically combining different predefined values, fine tuning as well the feature extraction stage (convolutional layers, batch normalization, and pooling) [42].

By combining the feature extraction with the abstract feature learning step (fully connected layers and dropout), the model is able to learn and extract the color correction intensity ($cci$), gamma correction ($\gamma$), $\alpha$ and $\beta$ values for the solution enhancement formula presented previously.

Color correction, gamma, brightness, and contrast intensities are indirectly influenced by the operations performed on the various CNN layers during training, as the network learns to represent and map image features to make increasingly accurate predictions. These parameters are obtained by previously application of intensity transformation techniques to the raw underwater images, subsequently the image processing steps can be performed from the CNN result.

### 3.2 Intensity Transformation Fusion

The process of obtaining empirically the best parameters consists of traversing the image and performing the processing steps, from various values in the scope of each technique. At each iteration the parameter values of color correction intensity ($cci$), gamma correction ($\gamma$), contrast intensity ($\beta$) and brightness intensity ($\alpha$) are defined, cycling through all possible combinations of parameter values. For each combination, a main function applies the image processing steps, and then the values of the quality metrics used for the image results are calculated (See the Subsection 4.3.1 for more details about the quality metrics).

Let $C = (cci_1, cci_2, ...)$ be the set of color correction intensity values, $G = (\gamma_1, \gamma_2, ...)$ be the set of gamma correction values, $A = (\alpha_1, \alpha_2, ...)$ be the set of alpha values and $B = (\beta_1, \beta_2, ...)$ be the set of beta values:

$$M = \left\{(cci_i, \gamma_j, \alpha_k, \beta_l) \,\middle|\, cci_i \in C, \gamma_j \in G, \alpha_k \in A, \beta_l \in B\right\}, \tag{9}$$

where $M$ is the set of combinations, $cci_i$ is a specific value from the set $C$, $\gamma_j$ is a specific value from the set $G$, $alfa_k$ is a specific value from the set $A$, and $\beta_l$ is a specific value from the set $B$.

This equation represents the Cartesian product of the sets $C$, $G$, $A$, and $B$, resulting in all possible combinations of parameter values for the image processing steps. Each combination represents a unique configuration of the parameters to be used in the processing.

If the quality metric values are desirable, the corresponding parameter combination is selected and the combination with the highest metric value is stored and prepared for labeling the images for the process of estimating these parameters for the test images and also for any images.

Below, we provide an overview of the mentioned techniques showcasing the step-by-step, from an input image (Fig. 4) to the correspondent restored image, while further in-depth information can be found in our previous paper [8].

#### 3.2.1 Color Correction

The first technique performed is a color correction algorithm, presented by Fig. 5, that applies histogram stretching in each color channel $(R, G, B)$. The technique takes all information from the linear curve minimum and maximum values, generating a 256 value Look-up Table to apply the histogram equalization. The image is scaled to $[min, max]$ range through a transformation of the pixel values by the function $f$, as in the equation below:

$$f(v) = (v - I^{min})(max - min)/(I^{max} - I^{min}) + min, \quad (10)$$

where $v$ is the gray value to be transformed, $I^{min}$ and $I^{max}$ correspond to the minimum and maximum gray values in the underwater image, respectively. $min$ and $max$ correspond to the new gray value range.

#### 3.2.2 Gamma Correction

The second technique is the gamma correction of underwater images, presented by Fig. 6. In this stage, the image pixel intensities are scaled from the range [0, 255] to [0, 1.0], by applying the equation:

$$I_G = I^{(1/g)}, \quad (11)$$

where $I$ is the underwater image and $g$ corresponds to the gamma constant value. $I_G$ is the underwater image with corrected gamma factor.

**Fig. 4** Raw Input Image

**Fig. 5** Color Correction Step

#### 3.2.3 Unsharp Enhancement

Figure 7 shows the final operation in each layer, the unsharp enhancement. For this step, the Unsharp Mask filter is used to enhance edges in underwater images. In this sense, it subtracts the smoothed version of the underwater image from its original underwater image, to highlight edges through the $h$ function. The mentioned process is performed as in the equation below:

$$h(v) = I(v) - I_{smooth}(v), \quad (12)$$

**Fig. 6** Gamma Correction Step

**Fig. 7** Image Sharpening Step

where $v$ is the gray value to be transformed, $I$ is an underwater image and $I_{smooth}$ corresponds to the smoothed underwater image.

#### 3.2.4 CLAHE

In this stage, visually represented by Fig. 8, the algorithm Contrast-Limited Adaptive Histogram Equalization (CLAHE) [43] is applied. This method operates on small regions of the image, called "tiles", in which the neighborhood pixels are combined using bilinear interpolation to remove the artificial boundaries. Thus, addressing and enhancing the image contrast. This evens out gray values distribution, making hidden features more visible. The expression of modified gray levels with Uniform Distribution is given by the equation below:

$$I_{he} = [I^{max} - I^{min}] * P(I) + I^{max}, \tag{13}$$

where $P$ is the cumulative probability distribution. $I^{min}$ and $I^{max}$ correspond to the minimum and maximum gray values in the underwater image, respectively. $I_{he}$ is the resulting underwater image after the histogram equalization process.

#### 3.2.5 Fusion

Let $I_1$ and $I_2$ be the processed underwater images in each layer of the proposed approach. $I_1$ and $I_2$ are combined using the linear blending as image fusion technique, represented by the $k$ function. Thereby, the visual features in $I_1$ and $I_2$ are fused in order to improve the quality and visibility of degraded underwater images. The linear blending operation was applied as below:

$$k(v) = (1 - \alpha)I_1(v) + \alpha I_2(v), \tag{14}$$

where $v$ is the gray value to be transformed, $\alpha$ represents the weight in the linear blending. $I_1$ and $I_2$ correspond to the processed underwater images in the first and second layers, respectively. Figure 9 provides a representation of the fusion step.

#### 3.2.6 Contrast and Brightness Adjustment

The generated fused underwater image undergoes brightness and contrast adjustment, and finally yields the final output of the proposed approach. To achieve brightness and contrast adjustment transformations, each output pixel value depends only on the corresponding input pixel value, by multiplication and addition with a constant. The parameters $\beta > 0$ and $\gamma$ control the contrast and brightness, respectively. The equation below presents the brightness and contrast transformation:

$$I_o = \beta * I + \gamma, \tag{15}$$

where $I$ is an underwater image, $\beta$ corresponds to the contrast factor and $\gamma$ corresponds to the brightness factor. $I_o$ is the output image in our approach for enhancement of underwater images, as can be seen in Fig. 10.

**Fig. 8** Contrast-Limited Adaptive Histogram Equalization Step

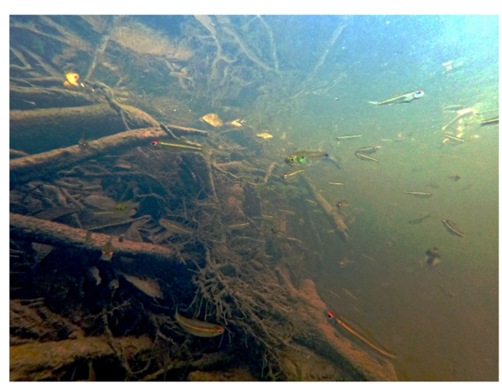

**Fig. 9** Fusion Step

**Fig. 10** Brightness and Contrast Adjustment Final Step

## 4 Experiments

This section evaluates the proposed approach, conducting both qualitative and quantitative assessments. The experimental evaluation involves the comparison of our approach with traditional methods as well as recent state-of-the-art techniques based on deep learning. These experiments allow us to evaluate the effectiveness of our method in restoring details, enhancing colors and improving the overall visual clarity, related to the comparison approaches.

The experiments were conducted using a Lenovo laptop with an Intel® Core$^{TM}$ i7-10750H CPU @ 2.60GHz, 16 GB DDR4-2133 main memory and NVIDIA® GeForce® RTX 3060 6 GB GDDR6. Furthermore, the OpenCV and Tensorflow frameworks were used to support the development of the proposed approach for underwater image restoration.

### 4.1 Experimental Datasets

The experiments were performed using two well-stated underwater image datasets, U45 and UIEB. These datasets comprise a collection of underwater images from the ocean and are commonly used in the literature [44, 45]. The U45 dataset consists of 45 images depicting natural underwater environments, while the UIEB dataset consists of 890 images capturing diverse natural underwater scenes. Both present reference images, enabling the comparative analysis and evaluation.

Figure 11 presents examples of underwater images, captured from the ocean, representing challenging subaquatic scenarios in different acquisition conditions and with different water aspects, affecting image quality and clarity. Figures 11a, b and c correspond to samples of underwater images from the U45 dataset. Figures 11d, e and f correspond to samples of underwater images from the UIEB dataset.

In this paper we introduce a collection of subaquatic images, called Amazon Underwater Image Dataset (AUID). The proposed AUID dataset consists of a challenging underwater image dataset, composed by 276 images from the Urubu river. The Urubu river is one of the tributaries of the Amazon river and is a major river in the Amazon Basin. The Urubu river plays a fundamental role in the overall hydrology and ecosystem of the Amazon region. The underwater images in the AUID dataset present high turbidity level, high scattering and low lighting in water, besides a dark color. Figure 12 presents examples of underwater images which comprise the AUID dataset.

### 4.2 Qualitative Evaluation

In this experiment we intend to assess the effectiveness of our proposed underwater image restoration technique in comparison to other existing techniques. In this evaluation, we examine the visual quality and perceptual improvements achieved by our approach in restoring underwater images in all scenes provided from the datasets. By comparing the results of our technique with those obtained from other comparison techniques, we aim at identifying differences in terms of image clarity, visibility and overall visual appearance. This qualitative evaluation provides valuable insights into the strengths and limitations of the proposed technique. Additionally, this evaluation strategy can be used as a fundamental step in validating the quality of the proposed approach for underwater image restoration.

In order to qualitatively evaluate the proposed approach, several existing techniques were implemented and used to restore underwater images. The U45 dataset was evaluated using the techniques: VRE [9], UDCP [10], IBLA [11], CBF [12], GDCP [13], UWCNN (UCNN) [14], WaterNet (WN) [15] and LI [16]. Figure 13 presents restored underwater images by our proposed approach and the comparison techniques, with respect to the U45 dataset, enabling the visual assessment of the subaquatic images. The same techniques listed earlier were used to evaluate the UIEB dataset. Figure 14 presents restored underwater images from the UIEB dataset by our proposed approach and the comparison techniques, enabling the visual assessment of the subaquatic images.

Our approach was also qualitatively evaluated using the proposed AUID dataset. For this, were considered the techniques: Histogram Equalization (HE) [46], UDCP [10], IBLA [11] and WN [15]. Figure 15 presents restored underwater images by our proposed approach and the comparison techniques, regarding the AUID dataset, enabling the visual assessment of the subaquatic images.

#### 4.2.1 Qualitative Analysis: Results Discussion

From the raw and the restored underwater images, obtained using the proposed approach and the comparison techniques, it is possible to evaluate the quality of the enhancement process. In Fig. 13, we can verify visual aspects regarding visibil-

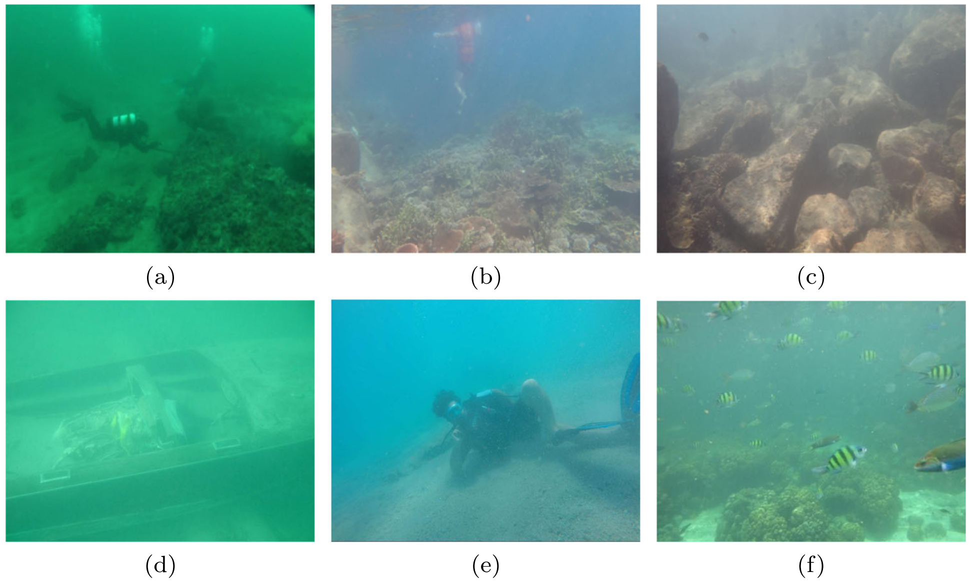


**Fig. 11** Samples representing subaquatic environments acquired from ocean, corresponding to U45 and UIEB datasets. Figure 11a, b and c represent scenes from U45 dataset. Figure 11d, e and f represent scenes from UIEB dataset

ity, clarity and colors, concerning the U45 dataset. Observing Fig. 13 we can see that some comparison techniques present quality results, like WN and LI. Nevertheless, aspects like high saturation, low turbidity reduction and excessive green and blue channel compensation affect the resulting underwater images. The IBLA method yields restored imkages highly saturated. The UCDP, IBLA, WN and LI methods does not reduce the turbidity properly in restored underwater images. Finally, the UCDP, IBLA and GDCP methods result in excessive green and blue channels compensation. Additionally, we can see that our approach presents significant results in the underwater scenes comprised in the U45 dataset.

In Fig. 14, we also can evaluate the quality of the restoration algorithms, comparing the visual and appearance aspects in raw and restored underwater images, in the UIEB dataset. From Fig. 14 it is possible to observe good visual results obtained using the comparison techniques VRE and LI. However, in some scenarios, degraded restored images are generated, like in UCDP, IBLA, GDCP, UCNN and WN methods, with an excessive green and blue channels compensation. The GDCP, CBF, LI and UCNN methods, do not reduce the turbidity in restoring process satisfactorily. Finally, the VRE, LI and CBF methods result in restored images with high saturation. Furthermore, we can verify the considerable performance of the proposed approach in the different underwater scenarios in the UIEB dataset.

Finally, in Fig. 15, it is possible to validate the performance of different underwater image restoration methods in a challenging subaquatic environment, with dark water, high turbidity and low visibility. From the visual analysis of the obtained results we can observe that, the comparison techniques presented unsatisfactory results, for the AUID dataset. The HE, UCDP and IBLA methods does not reduced significantly turbidity in restored images. The UCDP and WN methods yield images with low contrast, while the UCDP method generated underwater dark images. Our approach, regarding the proposed AUID dataset, achieved visually relevant results, especially due to the dataset difficulty, demonstrating the effectiveness of the proposed methodology, even in different subaquatic scenarios.

### 4.3 Quantitative Evaluation

In this experiment we intend to quantify the accuracy of the proposed approach for underwater image restoration. For this evaluation we have used measurements and metrics to

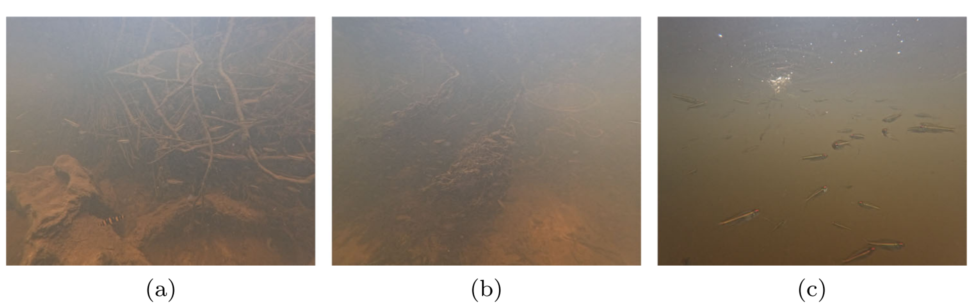


**Fig. 12** Samples representing subaquatic environments acquired from Urubu river, corresponding to AUID dataset. Figure 12a, b and c represent different scenes with intense turbidity and scaterring, also presenting low lighting aspect

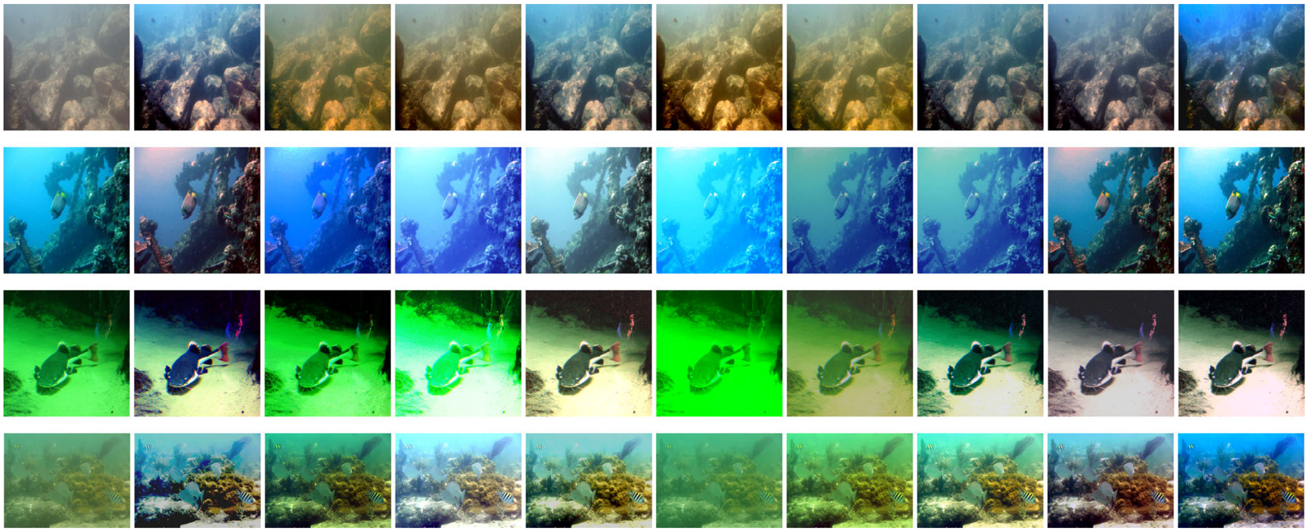

(a) Raws (b) VRE (c) UDCP (d) IBLA (e) CBF (f) GDCP (g) UCNN (h) WN (i) LI (j) Ours

**Fig. 13** Qualitative comparison of restored underwater images on U45 dataset. From left to right are presented the raw underwater images and the results of VRE, UDCP, IBLA, CBF, GDCP, UCNN, WN, LI and our method

quantitatively assess and compare the obtained results. From the numeric results it is possible to demonstrate the performance of our technique and the comparison algorithms. The employed metrics in this evaluation measure the quality, colorfulness, sharpness, contrast, entropy and the noise ratio from the restored underwater images, regarding different subaquatic datasets.

### 4.3.1 Evaluation Metrics

An image evaluation metric plays a fundamental role in assessing the quality and performance of image restoration techniques. Several metrics are commonly used, and in this experiment we have employed the UIQM (Underwater Image Quality Measure) [47], UISM (Underwater Image Sharpness Measure), UICONM (Underwater Image Colorfulness Measure), UICM (Underwater Image Contrast Measure), Entropy [48], PSNR (Peak Signal-to-Noise Ratio) [49], and SSIM (Structural Similarity Index) [50]. Each metric can estimate a different quality aspect in image, allowing a reliable comparison between several underwater image restoration techniques.

The UIQM is a non-reference image quality metric that combines multiple quality factors, including colorfulness ($c_1$), sharpness ($c_2$) and contrast ($c_3$), to provide an overall assessment of image quality. It takes into account both local

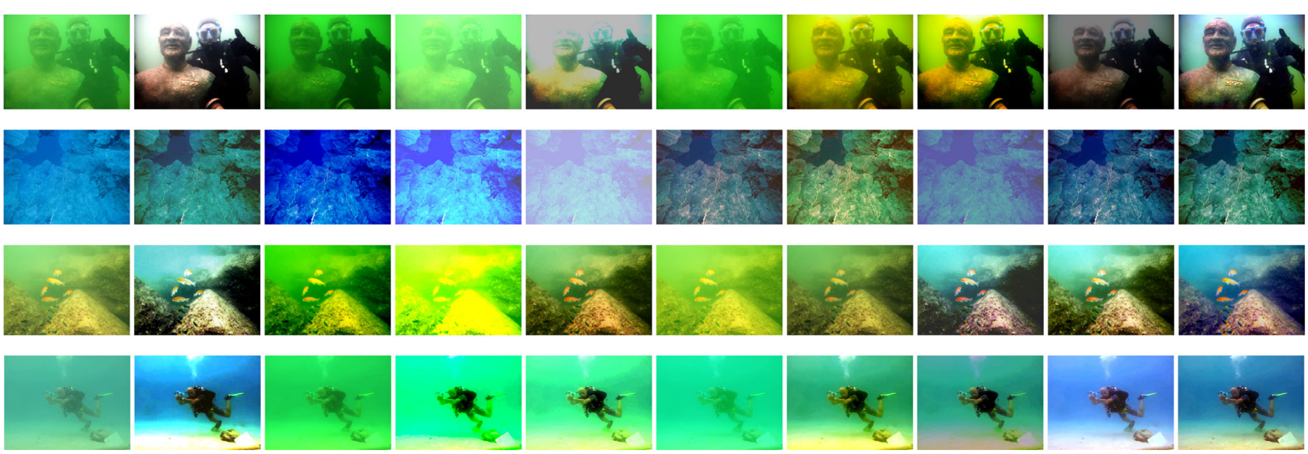

(a) Raws (b) VRE (c) UDCP (d) IBLA (e) CBF (f) GDCP (g) UCNN (h) WN (i) LI (j) Ours

**Fig. 14** Qualitative comparison of restored underwater images on UIEB dataset. From left to right are presented the raw underwater images and the results of VRE, UDCP, IBLA, CBF, GDCP, UCNN, WN, LI and our method

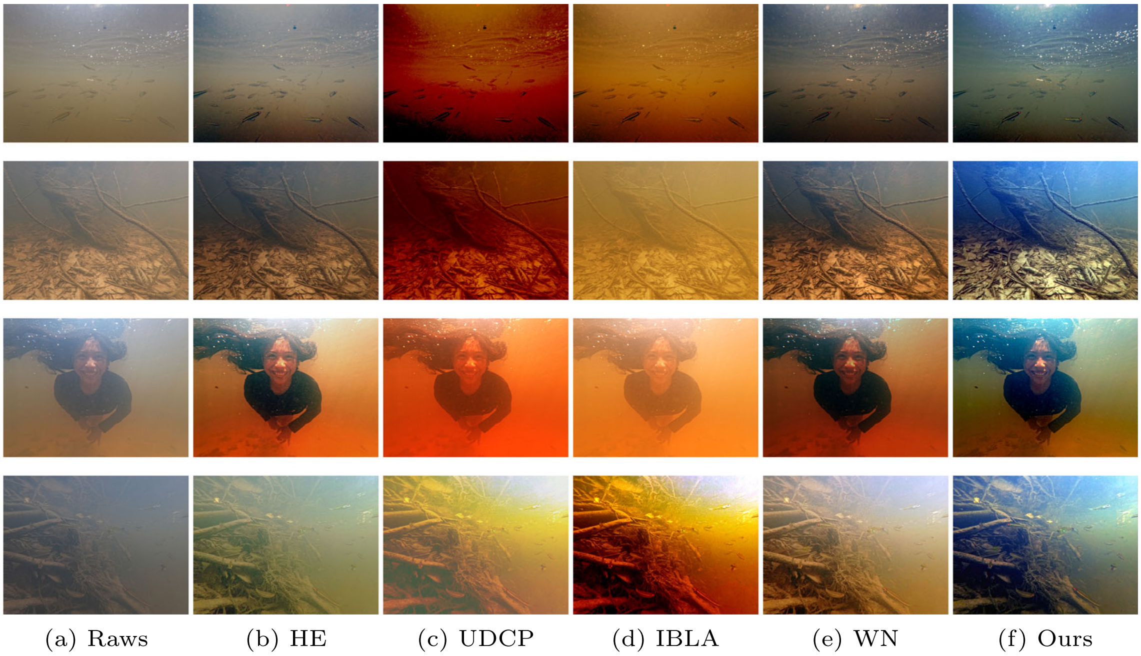


**Fig. 15** Qualitative comparison of restored underwater images on the proposed AUID dataset. From left to right are presented the raw underwater images and the results of HE, UDCP, IBLA, WN and our method

and global image features to measure the quality of underwater images. Every factor assess one aspect of the underwater image degradation and are linearly combined, as in:

$$UIQM = c_1{*}UICM{+}c_2{*}UISM{+}c_3{*}UICONM, \quad (16)$$

where the used weights in the experiments are: $c_1 = 0.468$, $c_2 = 0.274$, and $c_3 = 0.257$. In UIQM quality metric, the greater the result values mean, better the results.

The UISM, a non-reference image quality metric, focuses specifically on evaluating the sharpness of underwater images. The mentioned metric measures the local sharpness of edges and fine details, which are often degraded in underwater conditions. UISM is commonly used for assessing the restoration of important visual information, particularly the preservation and enhancement of fine details and edges.

In UICONM, a non-reference image quality metric, the colorfulness of underwater images is quantified. For this purpose, the method assesses the vibrancy and richness of color information, providing insights into the restoration of color in underwater scenes. UICONM is meaningful for evaluating the effectiveness of techniques in restoring and enhancing color fidelity, which is crucial for visual perception and interpretation.

The UICM, a non-reference image quality metric, evaluates the contrast in underwater images. It measures the difference in luminance between image regions, indicating the restoration of contrast and dynamic range. UICM helps to assess the effectiveness of techniques in enhancing visibility and revealing details that may be obscured in underwater conditions.

Entropy is a full reference image quality metric, that quantifies the amount of information or randomness present in an image. It measures the complexity and richness of image details and textures. Entropy is useful for evaluating the preservation of important visual information during the restoration process, as higher entropy values indicate better preservation of details.

The PSNR is a widely used full reference image quality metric, that calculates the ratio of the maximum possible signal power to the noise power. It quantifies the fidelity of the restored image compared to the original, with higher PSNR values indicating a closer resemblance. For this, in PSNR, from two images, an underwater image ($I$) and a reference underwater image ($R$), the Mean Squared Error ($MSE$) estimates the magnitude of the error, as in equation below:

$$MSE(I, R) = \frac{1}{N}\sum_{i=1}^{N}(I_i - R_i)^2, \quad (17)$$

where $N$ is the amount of pixels in the underwater image ($I$) and $i$ corresponds to every pixel in $I$.

Thereby, the PSNR measure is given by:

$$PSNR(I, R) = 10 * \log_{10} \frac{L^2}{MSE(I, R)}, \quad (18)$$

where $L$ is the reference image maximum pixel intensity value. The higher the PSNR compared to the reference image, the better the quality of the compressed, or reconstructed image.

SSIM, a full reference image quality metric, is a perceptual metric that measures the similarity between the restored and original images based on structural information. It takes into account factors such as luminance, contrast and structure. SSIM is advantageous because it considers human visual perception and provides a more holistic assessment of image quality. The aforementioned metrics enable us to objectively measure the quality, fidelity and accuracy of the restored underwater images. Providing reliable comparison strategy to quantify the performance and precision of the restoration methods.

#### 4.3.2 Quantitative Analysis: Results Discussion

In order to evaluate our approach and the comparison techniques we quantified the restored underwater image quality, using the image quality metrics described above. For better comprehension and visualization, the obtained results are divided into non-reference and full reference analysis. In the non-reference analysis the image quality metrics used are UIQM, UISM, UICONM and UICM. Meanwhile, in the full reference analysis the image quality metrics used are Entropy, PSNR and SSIM.

In the first quantitative analysis, regarding the U45 dataset, presented in the Table 1, we compare the proposed approach and the algorithms VRE, UDCP, IBLA, CBF, GDCP, UWCNN, WN and LI, using the non-reference image quality metrics. From the results in the Table 1, it was possible to verify that for the UIQM and UICONM metrics the WN and LI restoration techniques presented the best results among the comparison techniques. For the UISM metric the LI and IBLA restoration techniques presented the best results among the comparison techniques. For the UICM metric the WN, LI and IBLA restoration techniques presented the best results among the comparison techniques. It is important to highlight that the proposed approach overcome all the comparison techniques, in all image quality metrics, obtaining better results in the different aspects assessed by the image quality metrics.

In the full reference analysis, still regarding the U45 dataset, presented in the Table 2, it was possible to verify that for the Entropy metric the WN and LI restoration techniques presented the best results among the comparison techniques. For the PSNR metric the WN, LI and UWCNN restoration techniques presented the best results among the comparison techniques. For the SSIM metric the LI restoration technique presented the best result among the comparison techniques. As observed in the non-reference analysis, for the same dataset, the proposed approach for underwater image restoration also overcome the comparison techniques in full reference analysis, demonstrating the accuracy of our methodology.

In the second quantitative analysis, regarding the UIEB dataset, presented in the Table 3, we compare the proposed approach and the same algorithms used for U45 dataset, using the non-reference image quality metrics. From the results in the Table 3, it was possible to verify that for the UIQM metric the LI and VRE restoration techniques presented the best results among the comparison techniques. For the UISM metric the WN restoration technique presented the best result among the comparison techniques. For the UICONM and UICM metrics the LI restoration technique presented the best result among the comparison techniques. It is important to highlight that our approach overcome all the comparison techniques, even in a more challenging dataset, comprising more underwater degradation in images.

In the full reference analysis, still regarding the UIEB dataset, presented in the Table 4, it was possible to verify that for the Entropy metric the LI and VRE restoration techniques

**Table 1** Non-reference image quality assessment regarding UIQM, UISM, UICONM and UICM on U45 dataset images

| Method | UIQM ↑ | UISM ↑ | UICONM ↑ | UICM ↑ |
|---|---|---|---|---|
| Raw | 2.388 | 5.063 | 0.235 | 5.228 |
| VRE | 3.212 | 4.769 | 0.206 | 4.714 |
| UDCP | 3.934 | 3.272 | 0.239 | 5.418 |
| IBLA | 3.438 | 4.799 | 0.293 | 9.311 |
| CBF | 2.886 | 4.774 | 0.221 | 4.614 |
| GDCP | 2.704 | 3.503 | 0.302 | 4.06 |
| UWCNN | 3.725 | 3.976 | 0.296 | 9.252 |
| WN | 4.414 | 4.521 | 0.38 | 9.589 |
| LI | 4.636 | 5.283 | 0.399 | 9.649 |
| Ours | **4.998** | **5.891** | **0.4** | **10.735** |

**Table 2** Full reference image quality assessment regarding Entropy, PSNR and SSIM on U45 dataset images

| Method | Entropy ↑ | PSNR ↑ | SSIM ↑ |
|---|---|---|---|
| Raw | 6.144 | 17.215 | 0.538 |
| VRE | 6.597 | 22.405 | 0.786 |
| UDCP | 5.513 | 21.838 | 0.684 |
| IBLA | 6.963 | 25.674 | 0.567 |
| CBF | 5.458 | 22.424 | 0.794 |
| GDCP | 6.165 | 23.601 | 0.758 |
| UWCNN | 6.032 | 26.879 | 0.585 |
| WN | 7.278 | 26.386 | 0.554 |
| LI | 7.924 | 26.714 | 0.831 |
| Ours | **7.936** | **26.967** | **0.847** |

**Table 3** Non-reference image quality assessment regarding UIQM, UISM, UICONM and UICM on UIEB dataset images

| Method | UIQM ↑ | UISM ↑ | UICONM ↑ | UICM ↑ |
|---|---|---|---|---|
| Raw | 2.195 | 3.971 | 0.242 | 5.499 |
| VRE | 4.028 | 4.200 | 0.228 | 8.718 |
| UDCP | 3.735 | 5.065 | 0.204 | 7.073 |
| IBLA | 2.842 | 3.983 | 0.143 | 7.245 |
| CBF | 3.914 | 4.101 | 0.223 | 4.982 |
| GDCP | 3.476 | 4.503 | 0.284 | 4.351 |
| UWCNN | 3.725 | 5.484 | 0.287 | 6.222 |
| WN | 3.748 | 6.591 | 0.207 | 4.535 |
| LI | 4.089 | 5.542 | 0.309 | 9.367 |
| Ours | **4.690** | **6.757** | **0.318** | **11.489** |

presented the best results among the comparison techniques. For the PSNR metric the LI restoration technique presented the best result among the comparison techniques. For the SSIM metric the WN and GDCP restoration techniques presented the best results among the comparison techniques. As in the previous non-reference analysis, for the UIEB dataset, our approach for underwater image restoration also achieve high accuracy, overcoming the comparison techniques in full reference analysis.

Finally, in the third quantitative analysis, regarding the AUID dataset, presented in the Table 5, we compare the proposed approach and the algorithms HE, UDCP, IBLA and WN, using the non-reference image quality metrics. From the results in the Table 5, it was possible to verify that for the UIQM metrics the WN and IBLA restoration techniques presented the best results among the comparison techniques. For the UISM metric the WN restoration technique presented the best result among the comparison techniques and our approach. For the UICONM and UICM metrics the WN restoration technique presented the best result among the comparison techniques. It is important to highlight that our approach overcome almost all the comparison techniques, even in a very challenging dataset, with high turbidity and low visibility.

**Table 4** Full reference image quality assessment regarding Entropy, PSNR and SSIM on UIEB dataset images

| Method | Entropy ↑ | PSNR ↑ | SSIM ↑ |
|---|---|---|---|
| Raw | 6.939 | 19.856 | 0.633 |
| VRE | 7.627 | 21.277 | 0.654 |
| UDCP | 7.109 | 23.673 | 0.675 |
| IBLA | 7.348 | 20.142 | 0.653 |
| CBF | 7.423 | 26.785 | 0.740 |
| GDCP | 7.343 | 25.254 | 0.788 |
| UWCNN | 6.592 | 23.458 | 0.677 |
| WN | 7.166 | 25.157 | 0.785 |
| LI | 7.718 | 27.157 | 0.756 |
| Ours | **7.784** | **27.299** | **0.793** |

**Table 5** Non-reference image quality assessment regarding UIQM, UISM, UICONM and UICM on AUID dataset images

| Method | UIQM ↑ | UISM ↑ | UICONM ↑ | UICM ↑ |
|---|---|---|---|---|
| Raw | 3.125 | 3.434 | 0.209 | 3.125 |
| HE | 4.476 | 5.852 | 0.220 | 6.011 |
| UDCP | 3.636 | 5.672 | 0.204 | 4.331 |
| IBLA | 6.877 | 4.457 | 0.193 | 5.814 |
| WN | 6.754 | **6.877** | 0.272 | 9.879 |
| Ours | **7.700** | 6.826 | **0.396** | **12.344** |

In the full reference analysis, still regarding the AUID dataset, presented in the Table 6, it was possible to verify that for the Entropy, PSNR and SSIM metrics the WN restoration technique presented the best results among the comparison techniques. However, the proposed approach achieved higher accuracy in all scenarios, in a full reference analysis. Thereby, we can validate the robustness and accuracy of our approach in different scenarios, like ocean and river, and different underwater degradation aspects and intensities.

## 5 Conclusion and Future Work

This paper presented an approach to underwater image quality enhancement using deep learning and intensity transformation techniques for subaquatic robotics. A CNN was used for learning the best parameters needed for the image transformation functions, such as contrast adjustment, histogram equalization and gamma correction. By combining these transformations using the parameters found by the CNN, our approach achieved robust results as presented by the experiments.

The proposed approach comprises two main steps: (1) from a set of raw underwater images is carried out a training

**Table 6** Full reference image quality assessment regarding Entropy, PSNR and SSIM on AUID dataset images

| Method | Entropy ↑ | PSNR ↑ | SSIM ↑ |
|---|---|---|---|
| Raw | 4.037 | 17.522 | 0.300 |
| HE | 4.422 | 26.048 | 0.586 |
| UDCP | 4.787 | 25.897 | 0.411 |
| IBLA | 6.475 | 26.085 | 0.621 |
| WN | 7.100 | 27.087 | 0.662 |
| Ours | **7.1975** | **27.553** | **0.667** |

process in order to learn the best parameters to restore quality subaquatic images, regarding different scenarios and water conditions. For this, a regression convolutional neural network receives the training image set and estimates the best parameters for the underwater image enhancement. (2) From the best parameters, found through the learning process, the intensity transformation functions are applied to restore the subaquatic images.

We have carried out experiments in order to perform a qualitative and quantitative evaluation of the proposed approach. We have also performed a comparison to other eight existing techniques, namely VRE, UDCP, IBLA, CBF, GDCP, UWCNN, WN and LI. Several metrics were used such as UIQM, UISM, PSNR, SSIM, among others. Through the experiments it was possible verify that underwater images are strongly affected by high turbidity, low visibility, scatering and contrast, turning the underwater image restoration process a challenging task, specially regarding different subaquatic scenarios like ocean and river.

The results have shown that restoring underwater images in any subaquatic environment and water condition it is a nontrivial operation. The best comparison techniques obtained satisfactory quantitative results, however presented unsatisfactory restored underwater images in qualitative analysis. However, the proposed approach achieved high accuracy and visual quality underwater images, demonstrating consistency in the restoration process.

In this work we have created a new underwater image dataset, namely Amazon Underwater Image Dataset (AUID). The AUID dataset is composed by 276 images from the Urubu river, which is a blackwater tributary of the Amazon river. This dataset shows the potential for the acquisition and use of underwater images from the Amazon region, particularly the blackwater rivers.

There are two main contributions: (1) an effective deep learning-based approach for underwater image quality enhancement to be used by subaquatic robots and (2) a new underwater image dataset from a blackwater river in the Amazon region.

As future directions of this work we intend to investigate different approaches for underwater image restoration, like using High Dynamic Range (HDR). We also intend to expand the sets of underwater images in experimental process, in order to propose an invariant to water condition underwater image restoration technique, addressing the most of the subaquatic scenarios. We also intend to improve and significantly increase the number of images in our underwater dataset.

**Acknowledgements** This work was developed with support from Motorola, through the IMPACT-Lab R&D project at the Institute of Computing (IComp) of the Federal University of Amazonas (UFAM).

**Author Contributions** Laura A. Martinho was responsible for the general design and development of the learning-based underwater image restoration approach. João M. B. Cavalcanti, José L. S. Pio and Felipe G. Oliveira have supervised the work and conducted the writing and revision of the paper. Felipe G. Oliveira was also responsible for the Amazon Underwater Image Dataset (AUID) acquisition.

**Funding** Motorola

**Availability of data and material** Datasets should be made available upon the acceptance and publication.

## Declarations

**Conflicts of interest** The authors declare that there is no conflict of interest.

**Ethical Approval** Not applicable

**Consent to Participate** Not applicable

**Consent to Publish** Not applicable



## References

1. Luo, W., Duan, S., Zheng, J.: Underwater image restoration and enhancement based on a fusion algorithm with color balance, contrast optimization, and histogram stretching. IEEE Access **9**, 31792–31804 (2021)
2. Berman, D., Levy, D., Avidan, S., Treibitz, T.: Underwater single image color restoration using haze-lines and a new quantitative dataset. IEEE Trans. Pattern Anal. Mach. Intell. **43**(8), 2822–2837 (2021)
3. Han, J., Shoeiby, M., Malthus, T.J., Botha, E., Anstee, J., Anwar, S., Wei, R., Petersson, L., Armin, M.A.: Single underwater image restoration by contrastive learning. 2021 IEEE Int. Geoscience and Remote Sensing Symposium IGARSS, pp 2385–2388 (2021)
4. Sequeira, G., Mekkalki, V., Prabhu, J., Borkar, S., Desai, M.: Hybrid approach for underwater image restoration and enhancement. In: 2021 International Conference on Emerging Smart Computing and Informatics (ESCI), pp 427–432 (2021)
5. Ahamed, J., Abas, P.E., De Silva, L.: Role of restored underwater images in underwater imaging applications. Appl. Syst. Innovat. **4**, 11 (2021)

6. Hu, K., Zhang, Y., Weng, C., Wang, P., Deng, Z., Liu, Y.: An underwater image enhancement algorithm based on generative adversarial network and natural image quality evaluation index. J. Marine Sci. Eng. **9**(7) (2021)
7. Wang, Y., Guo, J., Gao, H., Yue, H.: Uiec$^2$-net: Cnn-based underwater image enhancement using two color space. Signal Process. Image Commun. **96**, 116250 (2021)
8. Martinho, L., Oliveira, F., Cavalcanti, J., Pio, J.: Underwater image enhancement based on fusion of intensity transformation techniques. In: Anais do XIV Simpósio Brasileiro de Robótica e XIX Simpósio Latino Americano de Robótica, (Porto Alegre, RS, Brasil), pp. 348–353, SBC (2022)
9. Fu, X., Zhuang, P., Huang, Y., Liao, Y., Zhang, X.-P., Ding, X.: A retinex-based enhancing approach for single underwater image. In: 2014 IEEE International Conference on Image Processing (ICIP), pp. 4572–4576 (2014)
10. Drews, P.L., Nascimento, E.R., Botelho, S.S., Montenegro Campos, M.F.: Underwater depth estimation and image restoration based on single images. IEEE Comput. Graphics Appl. **36**(2), 24–35 (2016)
11. Peng, Y.-T., Cosman, P.C.: Underwater image restoration based on image blurriness and light absorption. IEEE Trans. Image Process. **26**(4), 1579–1594 (2017)
12. Ancuti, C.O., Ancuti, C., De Vleeschouwer, C., Bekaert, P.: Color balance and fusion for underwater image enhancement. IEEE Trans. Image Process. **27**(1), 379–393 (2018)
13. Peng, Y.-T., Cao, K., Cosman, P.C.: Generalization of the dark channel prior for single image restoration. IEEE Trans Image Process. **27**(6), 2856–2868 (2018)
14. Li, C., Anwar, S., Porikli, F.: Underwater scene prior inspired deep underwater image and video enhancement. Pattern Recognit. **98**, 107038 (2020)
15. Li, C., Guo, C., Ren, W., Cong, R., Hou, J., Kwong, S., Tao, D.: An underwater image enhancement benchmark dataset and beyond. IEEE Trans. Image Process. **29**, 4376–4389 (2020)
16. Zhuang, P., Li, C., Wu, J.: Bayesian retinex underwater image enhancement. Eng. Appl. Artif. Intell. **101**, 104171 (2021)
17. Yang, H., Tian, F., Qi, Q., Wu, Q., Li, K.: Underwater image enhancement with latent consistency learning-based color transfer. IET Image Process. **16**, 1594–1612, 05 (2022)
18. Xing, Z., Cai, M., Li, J.: Improved shallow-uwnet for underwater image enhancement. In: 2022 IEEE International Conference on Unmanned Systems (ICUS), pp. 1191–1196 (2022)
19. Hu, K., Weng, C., Zhang, Y., Jin, J., Xia, Q.: An overview of underwater vision enhancement: From traditional methods to recent deep learning. J. Marine Sci. Eng. **10**(2) (2022)
20. Lyu, Z., Peng, A., Wang, Q., Ding, D.: An efficient learning-based method for underwater image enhancement. Displays **74**, 102174, 03 (2022)
21. Qiao, N., Dong, L., Sun, C.: Adaptive deep learning network with multi-scale and multi-dimensional features for underwater image enhancement. IEEE Trans. Broadcast. **69**(2), 482–494 (2023)
22. Huang, Y., Yuan, F., Xiao, F., Cheng, E.: Underwater image enhancement based on color restoration and dual image wavelet fusion. Signal Process.: Image Commun. **107**, 116797 (2022)
23. Sharma, P.K., Bisht, I., Sur, A.: Wavelength-based attributed deep neural network for underwater image restoration (2022)
24. Liu, S., Fan, H., Lin, S., Wang, Q., Ding, N., Tang, Y.: Adaptive learning attention network for underwater image enhancement. IEEE Robotics Automat. Lett. **7**(2), 5326–5333 (2022)
25. Wang, Y., Zhao, Y., Pan, H., Zhou, W.: An improved reinforcement learning method for underwater image enhancement. In: 2022 IEEE 25th International Conference on Computer Supported Cooperative Work in Design (CSCWD), pp. 1077–1082 (2022)
26. Fu, Z., Fu, X., Huang, Y., Ding, X.: Twice mixing: A rank learning based quality assessment approach for underwater image enhancement. Signal Process.: Image Commun. **102**, 116622 (2022)
27. Zhuang, P., Wu, J., Porikli, F., Li, C.: Underwater image enhancement with hyperlaplacian reflectance priors. IEEE Trans. Image Process. **31**, 5442–5455 (2022)
28. Zheng, M., Luo, W.: Underwater image enhancement using improved cnn based defogging. Electronics **11**(1) (2022)
29. Liu, Y., Xu, H., Zhang, B., Sun, K., Yang, J., Li, B., Li, C., Quan, X.: Model-based underwater image simulation and learning-based underwater image enhancement method. Information **13**(4) (2022)
30. F. L. C. L. D. D. J. A. Jiang, Li, Q.: Underwater imaging formation model-embedded multiscale deep neural network for underwater image enhancement. Math. Problems Eng. **13**(4) (2022)
31. Kai, Y., Lanyue, L., Ziqiang, Z., Guoqing, W., Yang, Y.: Medium transmission map matters for learning to restore real-world underwater images. (2022)
32. Zhao, W., Rong, S., Li, T., Feng, J., He, B.: Enhancing underwater imagery via latent low-rank decomposition and image fusion. IEEE J. Oceanic Eng. **48**(1), 147–159 (2023)
33. Dhandapani, V., Muniraj, M., Muniraj, I.: Fusion based underwater image enhancement and detail preserving. In: 2022 International Conference on Signal and Information Processing (IConSIP), pp. 1–5 (2022)
34. Zhang, W., Zhuang, P., Sun, H.-H., Li, G., Kwong, S., Li, C.: Underwater image enhancement via minimal color loss and locally adaptive contrast enhancement. IEEE Trans. Image Process. **31**, 3997–4010 (2022)
35. Preethi, B., Anuradha, C., Harshitha, I., Monika M.: Underwater image enhancement and super resolution based on deep cnn method. In: 2022 8th International Conference on Smart Structures and Systems (ICSSS), pp. 01–04 (2022)
36. Bapu, B.T., Partheeban, N., Nagaraju, V., Kumar, N.J., Ali, A.M.: Uips: A novel image resolution and clarity enhancement scheme for underwater image processing scheme. In: 2022 International Conference on Advances in Computing, Communication and Applied Informatics (ACCAI), pp. 1–7 (2022)
37. Gangisetty, S., Rai, R.R.: Floodnet: Underwater image restoration based on residual dense learning. Signal Processing: Image Commun. **104**, 116647 (2022)
38. Wang, L., Xu, L., Tian, W., Zhang, Y., Feng, H., Chen, Z.: Underwater image superresolution and enhancement via progressive frequency-interleaved network. J. Visual Commun. Image Represent. **86**, 103545 (2022)
39. Ren, T., Xu, H., Jiang, G., Yu, M., Zhang, X., Wang, B., Luo, T.: Reinforced swin-convs transformer for simultaneous underwater sensing scene image enhancement and superresolution. IEEE Trans. Geosci. Remote Sens. **60**, 1–16 (2022)
40. Wang, Y., Yu, X., Wei, Y., An, D., Bai, X.: Three-channel cascade network for underwater image enhancement. In: 2022 International Conference on High Performance Big Data and Intelligent Systems (HDIS), pp. 136–140 (2022)
41. Wang, S., Wang, D., Wang, E.: Improved underwater image enhancement model based on atomization images model and deep learning. In: 2022 IEEE 5th International Conference on Automation, Electronics and Electrical Engineering (AUTEEE), pp. 747–752 (2022)
42. LaValle, S.M., Branicky, M.S., Lindemann, S.R.: On the relationship between classical grid search and probabilistic roadmaps. Int. J. Robotics Res. **23**(7–8), 673–692 (2004)
43. Souza, J.R., Marchant, R., Ott, L., Wolf, D.F., Ramos, F.: Bayesian optimisation for active perception and smooth navigation. In: IEEE International Conference on Robotics and Automation (ICRA), pp. 4081–4087 (2014)

44. Li, C., Tang, S., Kwan, H.K., Yan, J., Zhou, T.: Color correction based on cfa and enhancement based on retinex with dense pixels for underwater images. IEEE Access **8**, 155732–155741 (2020)
45. Tao, Y., Dong, L., Xu, W.: A novel two-step strategy based on white-balancing and fusion for underwater image enhancement. IEEE Access **8**, 217651–217670 (2020)
46. Komal, V., Yaduvir, S.: Enhancement of images using histogram processing techniques. Int. J. Comput. Technol. Appl. **02**, 03 (2011)
47. Panetta, K., Gao, C., Agaian, S.: Human-visual-system-inspired underwater image quality measures. IEEE J. Oceanic Eng. **41**(3), 541–551 (2016)
48. Chen, X., Zhang, Q., Lin, M., Yang, G., He, C.: No-reference color image quality assessment: from entropy to perceptual quality. EURASIP J. Image Video Process. 2019 (2019)
49. Sara, U., Akter, M., Uddin, M.S.: Image quality assessment through fsim, ssim, mse and psnr—a comparative study. J. Comput. Commun. **07**, 8–18, 01 (2019)
50. Wang, Z., Bovik, A.C., Sheikh, H.R., Simoncelli, E.P.: Image quality assessment: from error visibility to structural similarity. IEEE Trans. Image Process. **13**, 600–612 (2004)



**Laura A. Martinho** is graduating in Computer Engineering from the University of Amazonas (UFAM), where she has been dedicated to her studies since 2019. Engaged in research and development projects, she has been an integral part of the IMPACT LAB (Laboratory of Computational and High-Performance Photography Technologies) since 2020, a collaborative project in computer vision between UFAM and Motorola.

**João M. B. Calvalcanti** received his Ph.D. degree in Artificial Intelligence from the University of Edinburgh in 2003. He also has a Master degree in Computer Science from the Federal University of Minas Gerais (UFMG) in 1995 and a degree of Bachelor in Data Processing from the Federal University of Amazonas (UFAM) in 1991. He is an Associate Professor at the Institute of Computing (IComp) at UFAM and his current research interests include information retrieval and image processing.

**José L. S. Pio** DSc. is a Professor of Computer Vision, Graphics and Robotics in the Computing Institute at Federal University of Amazonas. He holds B.S. degree in Civil Engineering from Federal University of Amazonas (1987), Master in Systems Engineering and Computing degree from COPPE/ UFRJ (1995), and Ph.D. degree in Computer Science from the Federal University of Minas Gerais (2006). Currently, he is a Full Associate Professor at the Federal University of Amazonas, affiliated with the Institute of Computing (ICOMP/UFAM) and the graduate programs in Informatics (PPGI) and the Graduate Program in Science and Mathematics Education (PPGECIM), He is the vice-president of the committee for the evaluation of scientific initiation projects in the exact sciences area, member of the Committee for the Evaluation of Scientific Initiation Projects in Engineering, and a member of the Ethics Committee in Scientific Research with Human Subjects at UFAM (CEP/UFAM). He is dedicated to undergraduate and graduate teaching in the fields of Discrete Event Systems Modeling and Simulation, Computer Graphics, Computer Vision, Intelligent Mobile Robotics, and Numerical Calculus. In scientific research, he is interested in the areas of Computer Vision, Computer Graphics and Robotics. He has previously coordinated and participated in research projects funded by CNPq, FAPEAM, and FINEP in the areas of Computer Vision and Mobile Robotics. He participates as a researcher and consultant in national and local interinstitutional projects focused on Computer Vision, Computer Graphics, and Intelligent Robotics.

**Felipe G. Oliveira** received the BSc degree in Computer Science from the Universidade Federal do Amazonas (UFAM) in 2009, and received the MSc degree in Informatics at the same institution in 2011. He received the PhD degree in Computer Science from the Universidade Federal de Minas Gerais (UFMG) in 2020. He has held a Visiting Scientist appointment at CSIRO in 2019. He is an Adjunct Professor at the Institute of Exact Sciences and Technology (ICET) at UFAM. Research interests include underwater image restoration for autonomous navigation of subaquatic robots, emphasizing obstacle detection, planning and mapping.